TRANSIENT MODELING OF A SMALL HYDROKINETIC TURBINE

J. R. P.Vaz[a],
T. H. S. Moreira[a],
D. T. Brandão[a],
J. J. A. Lopes[a],
S. W. O. Figueiredo[a],
A. L. A. Mesquita[a],
M. A. B. Galhardo[b],
and C. J. C. Blanco[c]

[a] Universidade Federal do Pará
Faculdade de Engenharia Mecânica
Bairro do Guamá
CP. 479, Belém, Pará, Brasil
jerson@ufpa.br
[b] Universidade Federal do Pará
Faculdade de Engenharia Elétrica
CP. 479, Belém, Pará, Brasil
[c] Universidade Federal do Pará
Faculdade de Engenharia Sanitária e Ambiental
CP. 479, Belém, Pará, Brasil

Received: September 08, 2015
Revised: October 10, 2015
Accepted: November 09, 2015

ABSTRACT

In recent years, great attention has been given to the study of hydrokinetic turbines for power generation. Such importance is due to the use of clean energy technology by using renewable sources. Therefore, this work aims to present a relevant methodology for the efficient design of horizontal-axis hydrokinetic turbines with variable rotational speed. This methodology includes the Blade Element Method (BEM) for determining the turbine power coefficient, since BEM is widely used in the hydrokinetic turbine design due to its good agreement with experimental data. In addition, the dynamic equation of the driveline is used, taking into account the BEM to provide the rotor hydrodynamic torque coupled with the drive train model, including the multiplier and the electric generator. In this case, the modeling of the whole system comprises the hydrodynamic information of the rotor, the mass-moment of inertia, frictional losses and electromagnetic torque imposed by the generator. The theoretical results were obtained for the transient rotational speed and compared with field data measured from small hydrokinetic turbine installed at the Arapiranga-Açu creek, which is located in the city of Acará, Pará, Brazil.

Keywords: hydrokinetic turbine, blade element method, dynamic modeling

NOMENCLATURE

C rotor blade chord length, m
d_M bearing pitch diameter, m
f_1 factor depending on the bearing design
F_β force dependent on the direction and magnitude of the applied loads, N
f_0 factor depending on the type of bearing and method of lubrication
f_t radial load factor
F_r radial load, N
G geometry factor
h radial clearance or axial clearance, in
i_{sq} electric current in one synchronous phase, A
J_{total} total mass-moment of inertia, kg.m^4
J_f fluid added mass, kg.m^4
J_{blade} blade mass-moment of inertia, kg.m^4
J_{hub} hub mass-moment of inertia, kg.m^4
J_L generator mass-moment of inertia, kg.m^4
J_{GT} belt mass-moment of inertia, kg.m^4
L disk length, in
L_{gen} length of the rotor generator, m
m_{gen} mass of the rotor generator, kg
n rotational speed, rpm
p number of pole pair
P_M output power, W
R radius of the hydrokinetic turbine, m
r rotational speed ratio
R_0 disk outer radius, in
R_i disk inner radius, in
R_{gen} radius of the rotor generator, m
R_{cil} radius of the hub cylinder
T_M driveline torque, N.m
T_T turbine torque, N.m
T_D dissipative torque, N.m
$T_{L\text{-}M}$ equivalent load torque, N.m
T_L generator torque, N.m
T_1 dependent component of friction torque, N.m
T_0 independent component of friction torque, N.m
T_v frictional torque, lbf.in

Greek symbols

ω_M angular speed of the rotor, rad/s
η multiplier efficiency
ω_L angular speed of the generator, rad/s
ω_M angular speed of the turbine, rad/s
ρ water density, kg/m^3
ψ magnetic flux, Wb
v_0 lubricant kinematic viscosity, m^2/s
μ lubricant absolute viscosity, lbf.s/in^2
ω_M disk angular speed, rad/s
η_{blade} number of blades

INTRODUCTION

This work develops a dynamic analysis of a small hydrokinetic turbine installed in the city of Acará, PA, which is part of the microregion called Tome-Açu, located at latitude 01º57'39" South and longitude 48º11'48"West (see Fig. 1a) and at an altitude of 25 m. It has an area of 4363,6 km² and a population of 53605 habitants (IBGE, 2008).The Arapiranga-Açu creek, shown in Figure 1b presents a velocity range of 0.1 to 1,2m/s, depending on the year season. Readings of stream velocity and turbine shaft rotational speed for the cases with and without electrical loading conditions were performed. After this step, it was done adaptation and application of the model developed by Mesquita et al. (2014) to the dynamic analysis of hydrokinetic turbines.

Figure 1. (a) Location of the creek; (b) Hydrokinetic turbine installed at Arapiranga-Açu.

The hydrokinetic turbine is an assembly of: (a) 4-blade rotor;(b) GÖ (Goetingen) 428/480 aluminum hydrofoil (480 on the tip and 428 on the base) of 60 cm diameter combined with a NACA 0012 airfoil; (c) Alternator (directly connected to the pulley of the mechanical transmission system). Its rated characteristics are: output power of 500 W, rotation of 900 rpm and output voltage of 12 V, model A116, transmission ratio of 1:4, adopting efficiency of 96.5%, according to Sarkis (1949). The greater pulley has a 400 mm diameter, while the smaller has a 100 mm diameter, and the clearance between shafts is 1265 mm.

DYNAMIC MODEL

A complete hydrokinetic turbine consists of a turbine rotor with mass moment of inertia J_T connected to a generator (electric load) with mass moment of inertia J_L through a gearbox with speed ratio r and efficiency η, as shown in Figure 2.

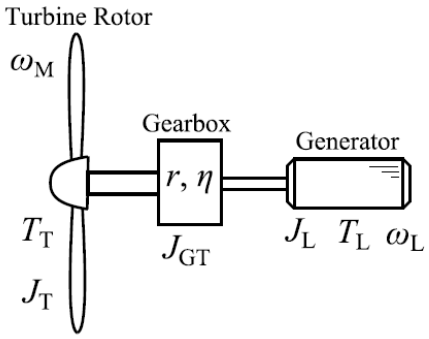

Figure 2. Illustration of the complete system of a hydrokinetic turbine.

The shafts and the gears are considered infinitely rigid. This assumption is valid since the vibration modes of the system are assumed to be in a frequency range far from the operational frequency. The dynamic equation governing the power transmission system shown in Figure 2 is given by:

$$T_M = T_T - T_D - T_{L-M} = J_{total}\frac{d\omega_M}{dt} \quad (1)$$

The driving torque (T_M) is equal to the torque of the turbine (T_T) minus the dissipative torque (T_D) (friction torques of bearings). ω_M is the angular speed of the rotor. The torque of the turbine is computed using hydrodynamic analysis. T_{L-M} is the equivalent load torque. Its expression is given by:

$$T_{L-M} = \frac{1}{\eta} r T_L \quad (2)$$

where T_L is the generator torque, η is the multiplier efficiency and r is the speed ratio $r = \omega_L / \omega_M$. The total mass-moment of inertia (J_{total}) is the sum of following parameters: inertia of the turbine (J_T); inertia of the fluid added mass around the rotor blades (J_f), inertia of the belt transmission with

respect to the input shaft of the multiplier (J_{GT}), and the inertia of the generator (J_L), i.e:

$$J_{total} = J_T + J_f + J_{GT} + J_L \quad (3)$$

In next subsections, the other terms in Eq. (1) and (3) are discussed in details. Finally, the rotor torque T_T can be expressed as:

$$T_T = \frac{P_M}{\omega_M} = \frac{1}{2}\frac{\rho\pi R^2 V^3}{\omega_M} C_P \quad (4)$$

Generator Torque

Hong et al. (2013) and Hasanien (2010) showed that the electricity generation systems are attracting great attention, since those can be operated with constant speed or variable speed operations using power electronic converters. The permanent magnet synchronous generator is a good option for the high performance in variable-speed including high efficiency and high controllability. In this case, the torque of a permanent magnet synchronous generator can be given through following algebraic equation:

$$T_L = \frac{3}{2} p\psi i_{sq} \quad (5)$$

where p is the pole pair number, ψ is the magnet flux and i_{sq} is the electric current in one of the synchronous phases.

In order to reduce the complexity of the electromagnetic torque equation, it is assumed that the relation between synchronous generator torque and its angular speed is given by an approximated linear equation (Bao and Ye, 2001). In this case, a first order linear function that describes the electromagnetic torque as a function of the generator angular speed is used, which is:

$$T_L = K_e \omega_e + K_{e0} \quad (6)$$

where K_e and K_{e0} are obtained by linear fit with experimental data.

Friction Torque

According to the loads acting on the bearings and the bearing types used throughout the driveline, it is possible to estimate the overall friction torque in the power train. Witte (1973) and Harris and Kotzalas (2006) empirically studied the running friction torque of tapered roller bearings, which resulted in Eq.(10) for radial loaded bearings:

$$T_{D,tapered} = 3{,}35\times10^{-11} G (n v_0)^{\frac{1}{2}} \left(f_t \frac{F_r}{K} \right)^{\frac{1}{3}} \quad (7)$$

where G is a geometry factor based on the internal dimensions of the bearing, n is the shaft rotational speed, v_0 is the lubricant kinematic viscosity, f_t is a radial load factor and F_r is the radial load. Palmgren (1959) separated the friction torque into a loading dependent component (T_1) and a load independent component (T_0) which is influenced by the viscous property of lubricant type, the amount of the lubricant employed and bearing speed. Thus, the total friction torque (in N.m) is given by Eq. (11):

$$T_{D,rolling} = T_0 + T_1 \quad (8)$$

where

$$T_1 = 10^{-3} \times f_1 F_\beta d_M \quad (9)$$

$$T_0 = 10^{-10} \times f_0 (n v_0)^{\frac{2}{3}} d_M^3 \quad (10)$$

where F_β depends on the magnitude and directions of the applied load, d_M is the bearing pitch diameter and f_0 is a factor depending on the type of bearing and the method of lubrication. More detail about those formulas can be found in Harris and Kotzalas (2006). Ker Wilson (1965) provides the following equation for the torque due to friction acting on all surfaces of a hollow disk:

$$T_v = \frac{\pi\mu\omega_M \left[R_0^3 + \left(R_0 + 2L \right) - R_i^4 \right]}{h} \quad (11)$$

where T_v is the frictional torque (in.lbf), μ is the fluid absolute viscosity (lbf.s/in^2), ω_M is the disk angular velocity (rad/s), R_0 is the disk outside radius (in), R_i is the disk inside radius (in), h is the radial clearance or axial clearance (assumed equal) (in) and L is the disk length (in).

Inertia Calculation

Turbine Rotor and Added Mass

The total rotor mass-moment of inertia is:

$$J_T = \eta_{blade} + J_{blade} + J_{hub} \quad (12)$$

where η_{blade} is the number of blades, J_{blade} is the blade mass-moment of inertia and J_{hub} is the hub mass-moment of inertia.

For the blade case, the mass-moment of inertia is calculated as following: the blade is divided into several small volumes along its length. At each volume the center of gravity is determined, as well as the mass and the distance between the mass center to the rotation center of the blade. Therefore, the

equation that provides the blade mass-moment of inertia is given by:

$$J_{blade} = \sum_{i=1}^{N} m_i r_i^2 + J_{root} = \sum_{i=1}^{N} m_i r_i^2 + m_{root} r_{root}^2 \quad (13)$$

The hub mass-moment of inertia has a geometry which can be approximated by a hollow hemisphere. Thus, the expression of its mass-moment of inertia is:

$$J_{hub} = \frac{3}{3} m_{hub} r_{hub}^2 \quad (14)$$

For the cube, the masses corresponding to the holes in the hub that should be subtracted. In the expression of the total mass-moment of inertia, the added mass of the fluid around the blades should also be taken into account. In the model described by Maniaci and Li (2011), the added mass was assumed to be equal to the mass of a cylinder (with length equal to the length of the blade, R) whose diameter is equal to the chord length C. Thus, the expression for the added mass is:

$$m_a = \pi R_{cil}^2 \rho L = \frac{1}{4} \pi C^2 \rho L \quad (15)$$

where R_{cil} is the radius of cylinder. In order to calculate the inertia of the fluid, it is proposed here the insertion of the added mass which can be calculated as:

$$J_{blade,fluid} = \sum_{i=1}^{N} \left(m_i + \frac{m_a}{N} \right) r_i^2 + J_{root} = \sum_{i=1}^{N} \left(m_i + \frac{m_a}{N} \right) r_i^2 + m_{root} r_{root}^2 \quad (16)$$

Therefore, the rotor mass-moment of inertia and the fluid added mass is given by:

$$J_T + J_f = \eta_{blade} J_{blade,fluid} + J_{hub} \quad (17)$$

Generator Inertia

The equivalent inertia of the generator ($J_{L\text{-}M}$) is:

$$J_{L\text{-}M} = \frac{1}{\eta} r^2 J_L \quad (18)$$

where J_L is the generator mass-moment of inertia, η is the multiplier efficiency and r is the speed ratio $r = \omega_L / \omega_M$. For J_L it was considered a cylinder of mass m_{gen}, radius R_{gen} and length L_{gen}, i.e:

$$J_L = \frac{1}{2} m_{gen} R_{gen}^2 = \frac{1}{2} \rho_{gen} \pi R_{gen}^4 L_{gen} \quad (19)$$

FIELD MEASUREMENTS

The hydrokinetic turbine used in this work is an adaptation of the Generation 3 hydrokinetic turbine designed by the Universidade de Brasilia (UNB). The difference between turbines can be seen in Fig. 3. This adaptation was done in a partnership between the Universidade Federal do Pará (UFPA) and UNB, in order to consider the technical availability of regional resources.

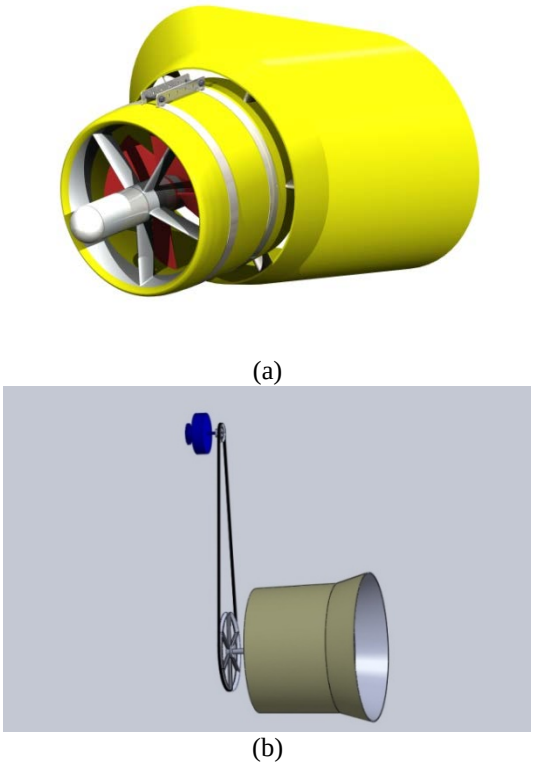

(a)

(b)

Figure 3. (a) Generation 3 hydrokinetic turbine designed by UNB; (b) Hydrokinetic turbine modified.

In this adaptation the design of the external structure and the machine power train were modified. The adjustments performed to the hydrokinetic turbine were: the transmission system has become belt driven and not by planetary gears as in the original one. The generator was incompatible with the reality of the water velocity at the Arapiranga-Açu creek, thus it was replaced by a permanent magnet generator, whose the main benefit are the operation at low shaft rotations; however, these generators usually have large dimensions as compared with conventional one. Therefore, the electrical generator was disconnected from the rotor

shaft, and placed outside of the water as illustrated in Figure 3b.

To measure the water velocity, it was used the Sontek Flow Tracker Adv. This equipment uses the Doppler effect, and is equipped with two probes which obtain speed data on the *x* and *y* reference axis. In this case, 10 measurements were performed. To collect data on the second shaft, a tachometer MINIPA, model MDT – 2238[a] (Figure 4) was used. The results of these measurements are presented in the next section of this work.

Figure 4. Shaft rotation measurements at the permanent magnet generator.

RESULTS AND DISCUSSION

Results of the Field Measurements

Table 1 shows the measurements done in field. Ten measurements of rotation were carried out for each situation: rotation with and without electrical loading on the second shaft. For the measurements it was used the contact type tachometer. The transmission ratio was 1:4, therefore the rotations on the turbine shaft are: 35 rpm (with electrical loading) and 44.13 rpm (without electrical loading). The water stream average velocity was 0.24 m/s as shown in Figure 5. It is noteworthy that the field survey was conducted only in steady-state for both cases with and without electrical load, due to the complexity to arrive at the locality, which is far from the town. Measurements for the transient behavior are being performed in order to considering the dynamic study more realistic, and will be presented in a future work. However, the results presented in this work are reasonable to demonstrate the transient behavior of the proposed methodology.

Table 1. Measurements data obtained at the Arapiranga-Açu creek.

Number of Measurements	Stream velocity (m/s)	Shaft rotation - (rpm) Without electrical load	Shaft rotation - (rpm) With electrical load
1	0.245	175	139
2	0.298	177	140.2
3	0.221	174.6	139.3
4	0.222	174.6	137.1
5	0.234	176.7	140
6	0.244	176.9	139.9
7	0.241	178.2	139.8
8	0.229	176.5	141.1
9	0.266	176.7	140.9
10	0.235	178.9	141
Standard deviation	0.0232	1.4379	1.1889

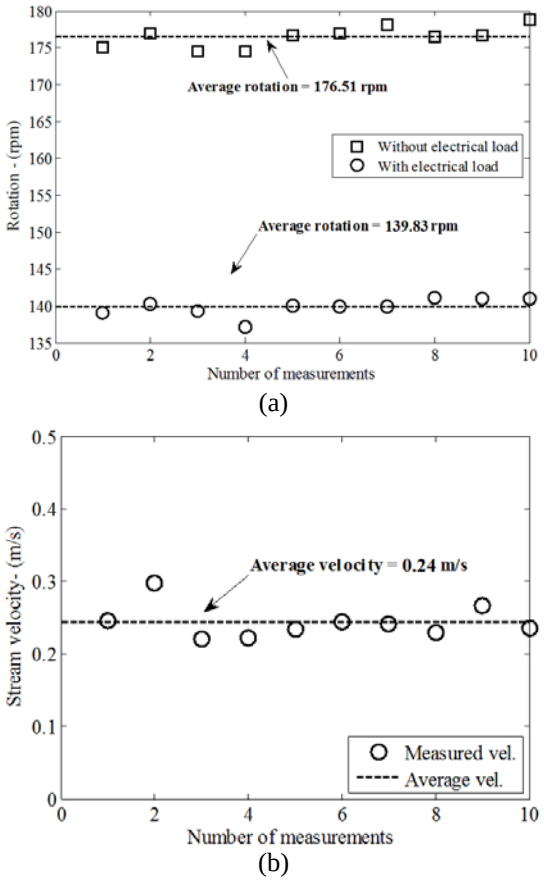

Figure 5. (a) Alternator shaft rotations and (b) stream velocities measured at Arapiranga-Açu creek.

Results of the Dynamic Model

Figure 6 shows values for the shaft rotation as a function of time using the dynamic model previously described. It is observed that in the curve region where the graph presents steady-state behavior, the result of the simulation is 3.55 rad/s. In this case, the relative error is 3.14% when compared to the mean values measured in field, shown in Figure 5. Such behavior confirm that the dynamic model has good concordance with the experimental results. An important effect, which should be considered in the hydrokinetic turbines design, corresponds to the behavior of the system when there is no electric charge. The rotational speed of the turbine increases abruptly due to the lack of electrical resistive torque. Thus, the elements that constitute the machine must be designed considering the effect of quick acceleration. In this case, shown in Figure 7, the numerical model has good agreement when compared with measured data, presenting error of 1.76%. The

present methodology has some limitations, which need to be investigated, as to take into account a detailed study of the starting condition of hydrokinetic turbines, and comparisons with shaft rotation dependents on time.

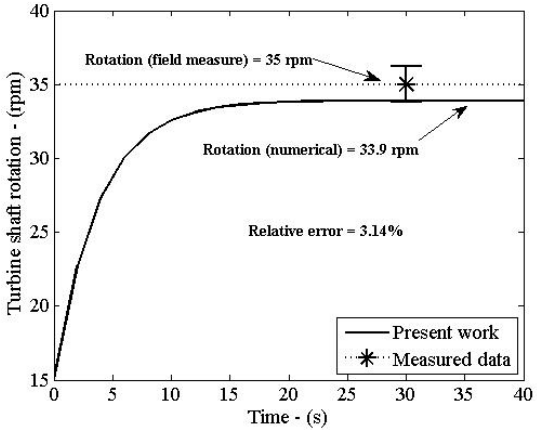

Figure 6. Rotation as a function of time - with electrical load.

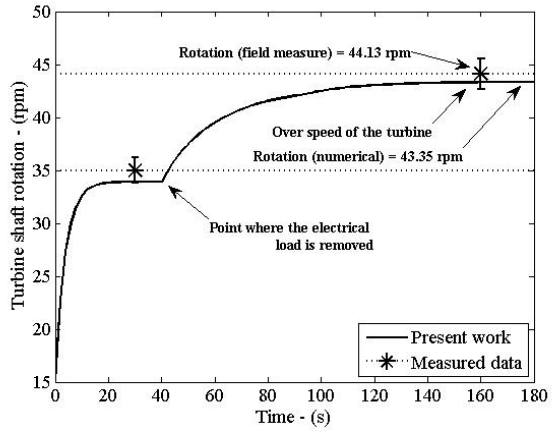

Figure 7. Rotation as a function of time - with and without electrical load.

CONCLUSIONS

In this paper, a comparison between the dynamic model proposed by Mesquita et al. (2014) and the field data measured at Arapiranga-Açu creek was performed. The analysis reveals good concordance and a relative error of 3.14%. Such result shows that the dynamic model described here is a useful tool for the efficient design of horizontal-axis hydrokinetic turbines. Clearly, the methodology represents an alternative approach, which consider the inertial effects and energy loss in the whole power system. This method solves the dynamic equation, using a scheme with low computational cost and easy implementation. An important aspect of this methodology is the use of the classical BEM method, which is applied at each time step in order to calculate the hydrodynamic torque of the turbine. This process is not current available in the literature, being an important contribution of this work. However, it is noteworthy that more investigation on the numerical model and more measurements for greater values of stream velocity are necessary in order to enlarge the range of results. The main limitations found here were: (a) the dissipative torque model is not applied to the starting condition. It is believed that the dissipative torque model needs modifications; (b) the data acquisition needs to be done for shaft rotation dependent on time.

ACKNOWLEDGEMENTS

The authors would like to thank CNPq, CAPES, PROPESP-UFPA, and ELETRONORTE for financial support.

REFERENCES

Bao, N., and Ye, Z., 2001, Active Pitch Control in Larger Scale Fixed Speed Horizontal Axis Wind Turbine Systems, Part I. Linear Controller Design, Wind Engineering, Vol. 25, No. 6, pp. 339-999.

Harris, T. A., and Kotzalas, M. N., 2006, *Essential Concepts of Bearing Technology*, 5th Edition, CRC Press.

Hasanien, H. M., 2010, Torque Ripple Minimization of Permanent Magnet Synchronous Motor using Digital Observer Controller, Energy Conversion and Management, Vol. 51, pp. 98-104.

Hong, C. M., Chen, C. H., and Tu, C. S., 2013, Maximum Power Point Tracking-Based Control Algorithm for PMSG wind Generation System without Mechanical Sensors, Energy Conversion and Management, Vol. 69, pp. 58-67.

Ker Wilson W., 1956, *Practical Solution of Torsional Vibration Problems*, 3rd Edition, John Wiley and Sons.

Maniaci, D. C., and Li, Y., 2011, Investigating the Influence of the Added Mass Effect to Marine Hydrokinetic Horizontal-Axis Turbines using a General Dynamic Wake Wind Turbine Code, in: *Oceans 11 - Conference Kona*, Hawaii, pp. 19-21.

Mesquita, A. L. A, Vaz, J. R. P., Morais, M. V. G., and Gonçalves, C., 2014, A Methodology for the Transient Behavior of Horizontal Axis Hydrokinetic Turbines, Energy Conversion and Management, Vol. 87, pp. 1261-1268.

Palmgren, A., 1959, *Ball and Roller Bearing Engineering*, 3rd Edition, Burbank, Philadelphia.

Sarkis, Melconian, 2000, *Elementos de Máquinas*, 7ª Ed., São Paulo, Érica. *(in Portuguese)*

Witte, D., 1973, Operating Torque of Tapered Roller Bearings, ASLE Transactions, Vol. 16, No. 1, pp. 61-67.